SUPPLEMENTARY FIGURES

Figure S1

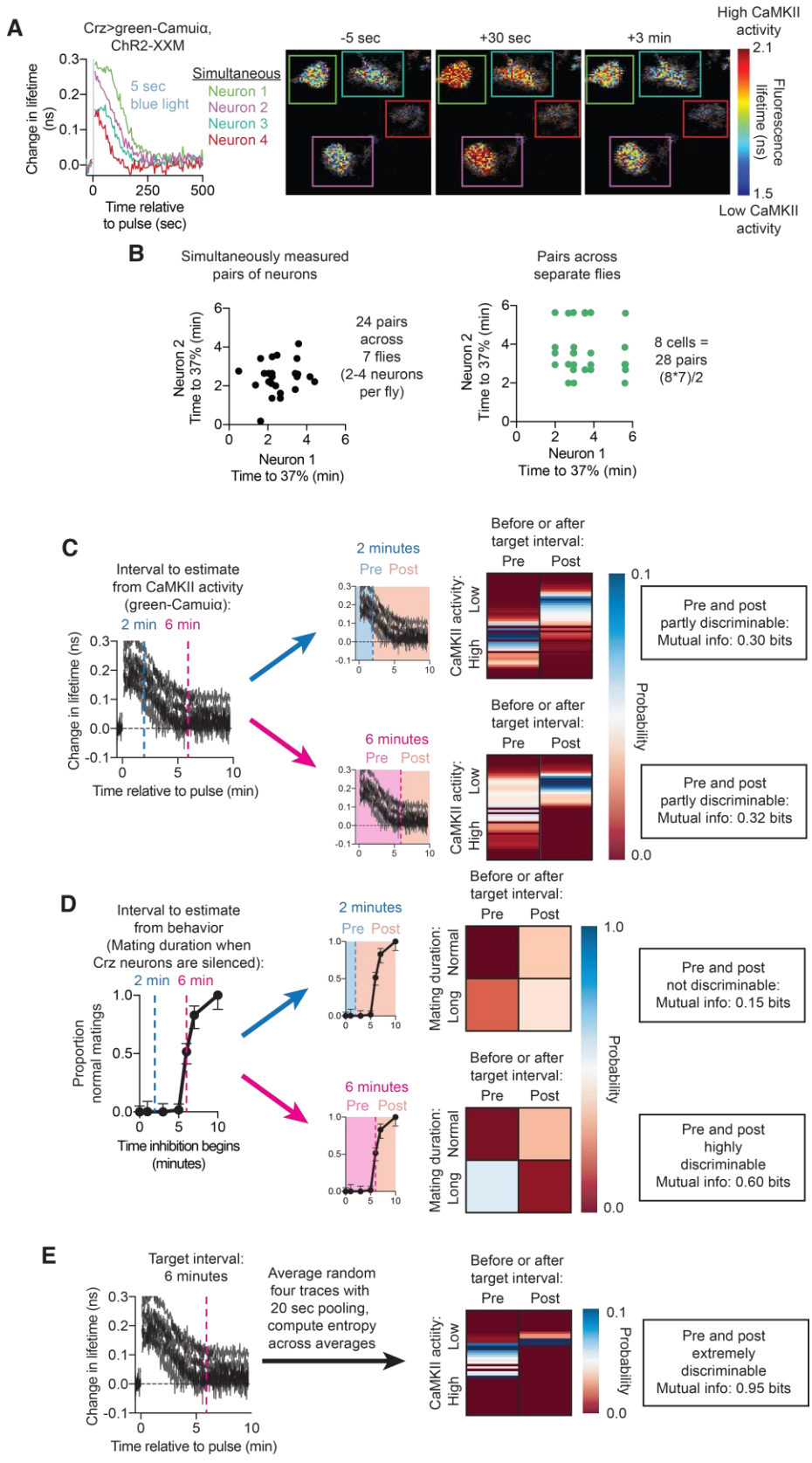
A
Crz>green-Camuia, ChR2-XXM
Change in lifetime (ns)
5 sec blue light
Simultaneous
Neuron 1
Neuron 2
Neuron 3
Neuron 4
Time relative to pulse (sec)
-5 sec
+30 sec
+3 min
High CaMKII activity
Fluorescence lifetime (ns)
Low CaMKII activity
B
Simultaneously measured pairs of neurons
Neuron 2 Time to 37% (min)
Neuron 1 Time to 37% (min)
24 pairs across 7 flies (2-4 neurons per fly)
Pairs across separate flies
8 cells = 28 pairs (8*7)/2
C
Interval to estimate from CaMKII activity (green-Camuia):
2 min 6 min
Change in lifetime (ns)
Time relative to pulse (min)
2 minutes
Pre Post
6 minutes
Pre Post
Before or after target interval:
Pre Post
CaMKII activity: Low High
Probability
Pre and post partly discriminable: Mutual info: 0.30 bits
Pre and post partly discriminable: Mutual info: 0.32 bits
D
Interval to estimate from behavior (Mating duration when Crz neurons are silenced):
2 min 6 min
Proportion normal matings
Time inhibition begins (minutes)
2 minutes
Pre Post
6 minutes
Pre Post
Before or after target interval:
Pre Post
Mating duration: Normal Long
Probability
Pre and post not discriminable: Mutual info: 0.15 bits
Pre and post highly discriminable Mutual info: 0.60 bits
E
Target interval: 6 minutes
Change in lifetime (ns)
Time relative to pulse (min)
Average random four traces with 20 sec pooling, compute entropy across averages
Before or after target interval:
Pre Post
CaMKII activity: Low High
Probability
Pre and post extremely discriminable Mutual info: 0.95 bits

Figure S1 (Related to Figure 1): Simultaneously measured CaMKII timers do not report exactly the same interval.

A) Green-Camuiα fluorescence lifetime in individual Crz neurons after optogenetic stimulation. Four simultaneously measured CaMKII timers show high variability relative to the mean decay time of CaMKII.

B) Decay kinetics of green-Camuiα activity in individual neurons compared against one another. The variability of simultaneously measured CaMKII timers (left) is comparable to the variability of CaMKII timers across neurons from separate flies (right), arguing that each neuron's CaMKII timer is independently set.

C) Eight independently measured CaMKII timers in separate animals after 7 seconds of optogenetic stimulation of the Crz neurons (Thornquist et al., 2020). To compute the mutual information between CaMKII activity and the passage of a particular interval of time (for example, 2 or 6 minutes), the population of CaMKII responses were split into two epochs: pre and post that interval. The probability density of CaMKII activity in each epoch was computed by binning the green-Camuiα fluorescence lifetime values into 0.02 nanosecond bins. These probability distributions were then used to quantify the entropy of the conditional distribution $p(\text{Interval has elapsed} \mid \text{CaMKII activity})$. This was compared to the entropy of the uninformed $p(\text{Interval has elapsed})$ in a 10-minute period (i.e. the length of the interval divided by 10 minutes) to compute the mutual information.

D) To compute the precision of the actual Crz network, we used data in which the Crz neurons were silenced using GtACR1 beginning at various times into mating. If the network has reached consensus by the onset of inhibition, flies will mate for a normal duration(Thornquist et al., 2020). Otherwise, they will mate for hours (long mating). For each target interval,
$p(\text{Interval has elapsed} \mid \text{a fly mates for a long time when the Crz neurons are inhibited})$ was computed and compared to $p(\text{Interval has elapsed})$ as in **Figure S1C**.

E) As in **D**, but averaging across four neurons at a time.

Figure S2

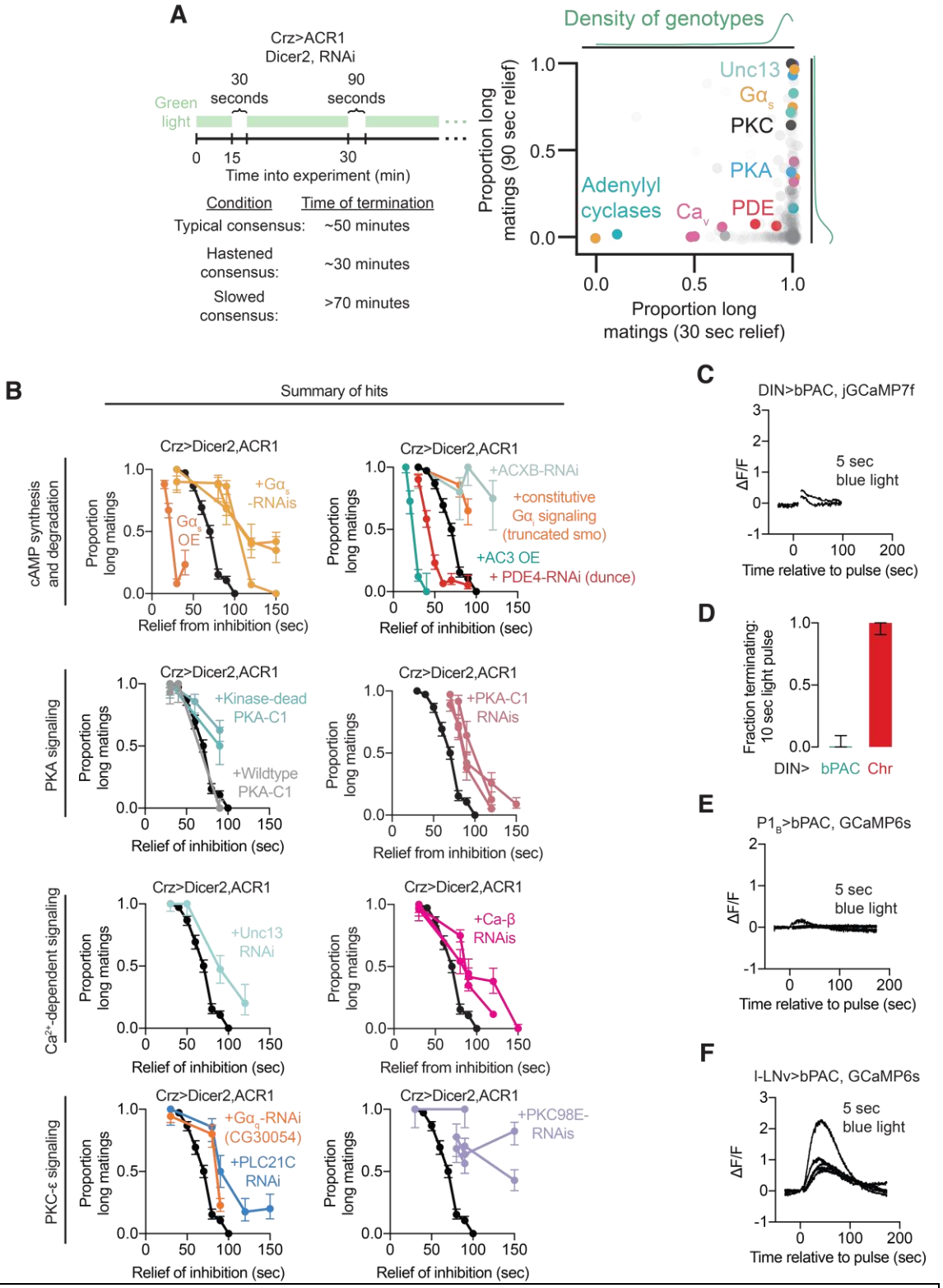

Figure S2 (Related to Figures 2 and 3): Further details of the screen for the mechanism of the consensus period and effects of bPAC on other populations of neurons

A) Left: Flies expressing GtACR1 in the Crz neurons, in addition to an RNAi knockdown or overexpression of a single gene, were exposed to two bouts of relieved inhibition: one 30 seconds long, and one 90 seconds long fifteen minutes later. Flies with no genetic modifications other than expression of GtACR1 will persist through the first bout without the Crz neurons reaching consensus, but will respond to the second bout by terminating mating 15-20 minutes later. If the consensus period is shortened by a manipulation, flies will terminate the mating ~18 minutes after the first period of relieved inhibition. If the consensus period is lengthened, flies will not stop mating even 20 minutes after the second bout.
Right: All 1,388 manipulations screened. Most hits were in the canonical cAMP signaling pathway, but we also hit the “novel” Protein Kinase C PKC98E pathway. Opacity of each point increases with sample size (genotypes with more data appear darker in the plot).
B) Characterization of hits from the screen (with multiple RNAi lines) by plotting the proportion of long matings in response to different durations of relieved inhibition. Each dot represents an independent cohort tested with a different duration period of relieved inhibition.
C) jGCaMP7f (used because GCaMP6s did not express well) fluorescence in the DINs after stimulation of bPAC. Stimulation of cAMP synthesis in the DINs (Drive Integrating Neurons (Thornquist and Crickmore, 2020), labeled by the line NP2719-Gal4 in Crickmore and Vosshall (Crickmore and Vosshall, 2013)) drives only a modest elevation in intracellular calcium.
D) Electrical excitation of the DINs with CsChrimson results in immediate termination of mating, while stimulation with bPAC has no effect.
E) GCaMP6s fluorescence in the P1 neurons after stimulation of bPAC. Stimulation of cAMP synthesis in the courtship-promoting P1 neurons (Kohatsu et al., 2011; von Philipsborn et al., 2011) has no effect on intracellular calcium.
F) GCaMP6s fluorescence in the l-LNvs after stimulation of bPAC. Stimulation of cAMP synthesis in the circadian large lateral ventral neurons (l-LNvs) (Shang et al., 2008) does result in significant rise in calcium, though the increase is much slower and of lower magnitude than in the Crz neurons. This is consistent with the large and rapid increase in calcium in response to bPAC activation in the Crz neurons coming from a threshold nonlinearity between cAMP signaling and calcium. Repeated weak stimulation of the l-LNvs does not show an accumulation-to-threshold or eruption-like effect.

Figure S3

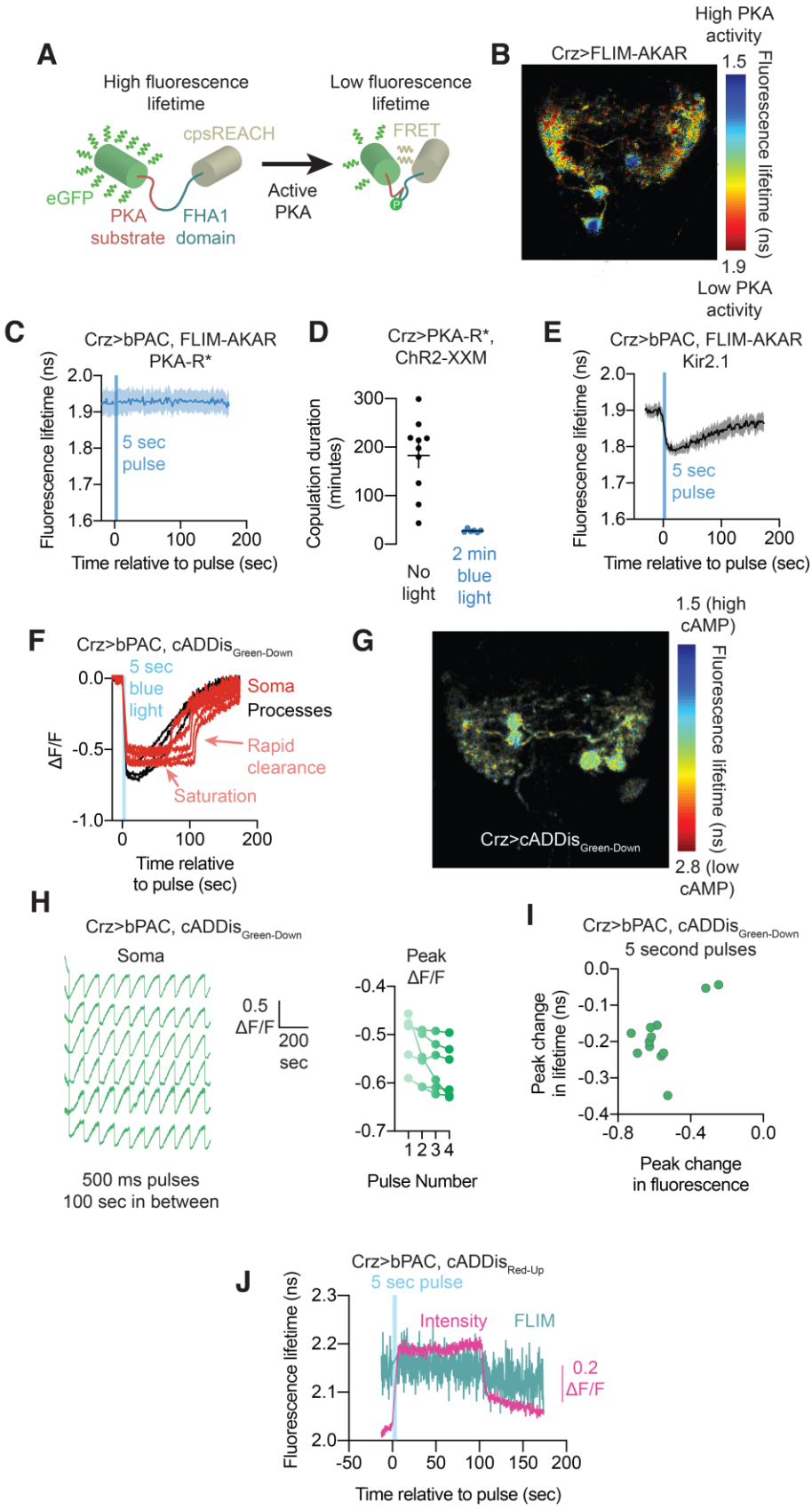
A
High fluorescence lifetime
Low fluorescence lifetime
cpsREACH
FRET
eGFP
PKA substrate
FHA1 domain
Active PKA
B
Crz>FLIM-AKAR
High PKA activity
1.5
Fluorescence lifetime (ns)
1.9
Low PKA activity
C
Crz>bPAC, FLIM-AKAR PKA-R*
Fluorescence lifetime (ns)
5 sec pulse
Time relative to pulse (sec)
D
Crz>PKA-R*, ChR2-XXM
Copulation duration (minutes)
No light
2 min blue light
E
Crz>bPAC, FLIM-AKAR Kir2.1
Fluorescence lifetime (ns)
5 sec pulse
Time relative to pulse (sec)
F
Crz>bPAC, cADDis Green-Down
5 sec blue light
Soma
Processes
Rapid clearance
Saturation
ΔF/F
Time relative to pulse (sec)
G
Crz>cADDis Green-Down
1.5 (high cAMP)
Fluorescence lifetime (ns)
2.8 (low cAMP)
H
Crz>bPAC, cADDis Green-Down
Soma
0.5 ΔF/F
200 sec
500 ms pulses
100 sec in between
Peak ΔF/F
Pulse Number
I
Crz>bPAC, cADDis Green-Down
5 second pulses
Peak change in lifetime (ns)
Peak change in fluorescence
J
Crz>bPAC, cADDis Red-Up
5 sec pulse
Intensity
FLIM
0.2 ΔF/F
Fluorescence lifetime (ns)
Time relative to pulse (sec)

Figure S3 (Related to Figure 4): Additional information related to PKA, cAMP, and corresponding reporters in the Crz neurons

A) Phosphorylation of a PKA substrate results in a conformation change of FLIM-AKAR, permitting non-radiative decay of eGFP excitation through FRET (Chen et al., 2014). This is read out as a reduction in fluorescence lifetime, providing a measurement of absolute levels of PKA signaling.
B) FLIM-AKAR expresses stably throughout the neuron and reveals variation in baseline levels of cAMP within the Crz neurons. Somas show much higher levels of basal PKA activity than the processes, though the dynamics in response to optogenetic induction of cAMP synthesis using bPAC are comparable.
C) FLIM-AKAR fluorescence lifetime in response to stimulation of bPAC in the presence of PKA-R*. Expression of the dominant negative PKA regulatory subunit PKA-R* completely blocks phosphorylation of FLIM-AKAR after stimulation of cAMP synthesis by bPAC.
D) Copulation duration of flies expressing PKA-R* in the Crz neurons with and without optogenetic stimulation using ChR2-XXM Stimulation of the Crz neurons reverts the effects of expression of PKA-R* on copulation duration.
E) FLIM-AKAR fluorescence lifetime in response to stimulation of bPAC in the presence of Kir2.1. Electrical inhibition of the Crz neurons using Kir2.1 does not prevent cAMP-induced activation of PKA, despite the absence of changes in intracellular calcium (**Figure 3H**).
F) cADDis$_{\text{Green-Down}}$ reports large changes in cAMP after strong (5 second) stimulation of bPAC that persists for over 100 seconds. At ~100 seconds – right at the time that the resultant eruption from optogenetic stimulation begins to end – somatic measurements of cAMP show extremely rapid clearance and return to baseline, suggesting the eruption triggers an active mechanism for cAMP clearance.
G) Baseline cAMP levels are higher in the soma than in the processes of the Crz neurons, as reported by fluorescence lifetime imaging of cADDis$_{\text{Green-Down}}$.
H) Individual cell traces from data reported in **Figure 4E**.
I) cAMP responses in the arbors of the Crz neurons show similar dynamics to the soma, though with less pronounced saturation at the peak of stimulation (likely due to the lower baseline before stimulation).
K) cADDis$_{\text{Red-Up}}$ shows no change in fluorescence lifetime with cAMP binding.

Figure S4

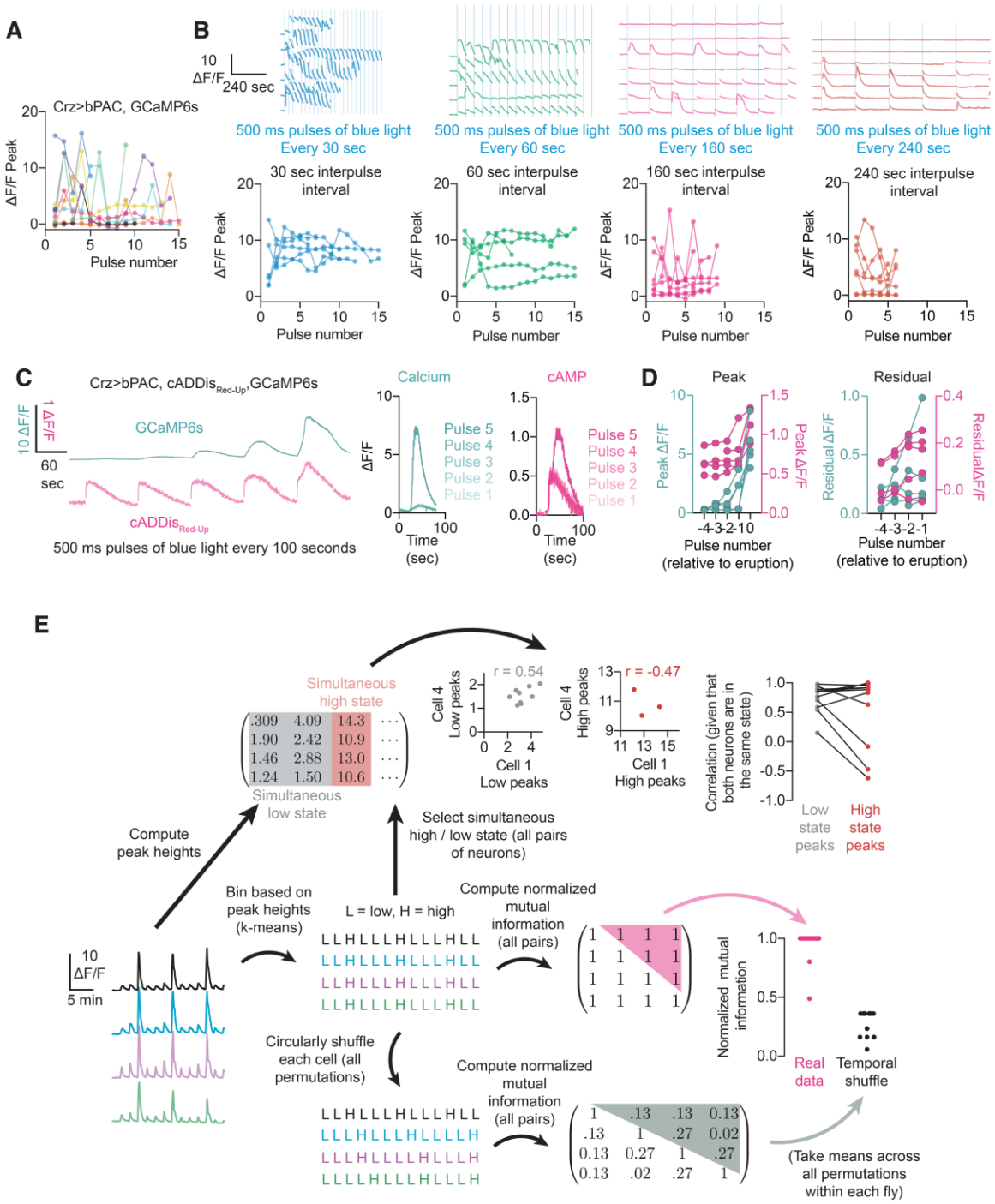

Figure S4 (Related to Figures 4 and 5): Changing the rate of cAMP accumulation changes the frequency of eruptions.

A) Responses from individual neurons in **Figure 4G** are replotted in different colors for comparison of peak heights.
B) Top: Increasing the frequency of bPAC stimulation eruptions, while further spacing the pulses causes less frequent eruptions. Bottom: Sequential eruptions neither increase

nor decrease in magnitude, suggesting that the eruption results from a saturating nonlinearity.

C) Simultaneous imaging of cAMP ($cADDis_{Red\text{-}Up}$) and calcium dynamics (GCaMP6s) in an individual Crz neuron shows the relationship between accumulating cAMP and eruptions.

D) Peak and residual levels of calcium and cAMP during the same experiment across multiple flies.

E) The peak response in the raw fluorescence data to each optogenetic impulse was binned into two bins, either a high response or a low response, by using 2-means clustering. The mutual information of this binarized classification was computed across all stimulations, and was compared to the mutual information of a circularly permuted distribution of high and low classifications (to preserve the tendency of multiple low peaks to precede each high peak, but allow the timing of each high peak for each cell to be misaligned to that of the others). The absolute magnitude of the low peaks was highly correlated, likely due to the recurrence of the Crz neurons, while the magnitude of the size of eruptions was sometimes less correlated.

Figure S5

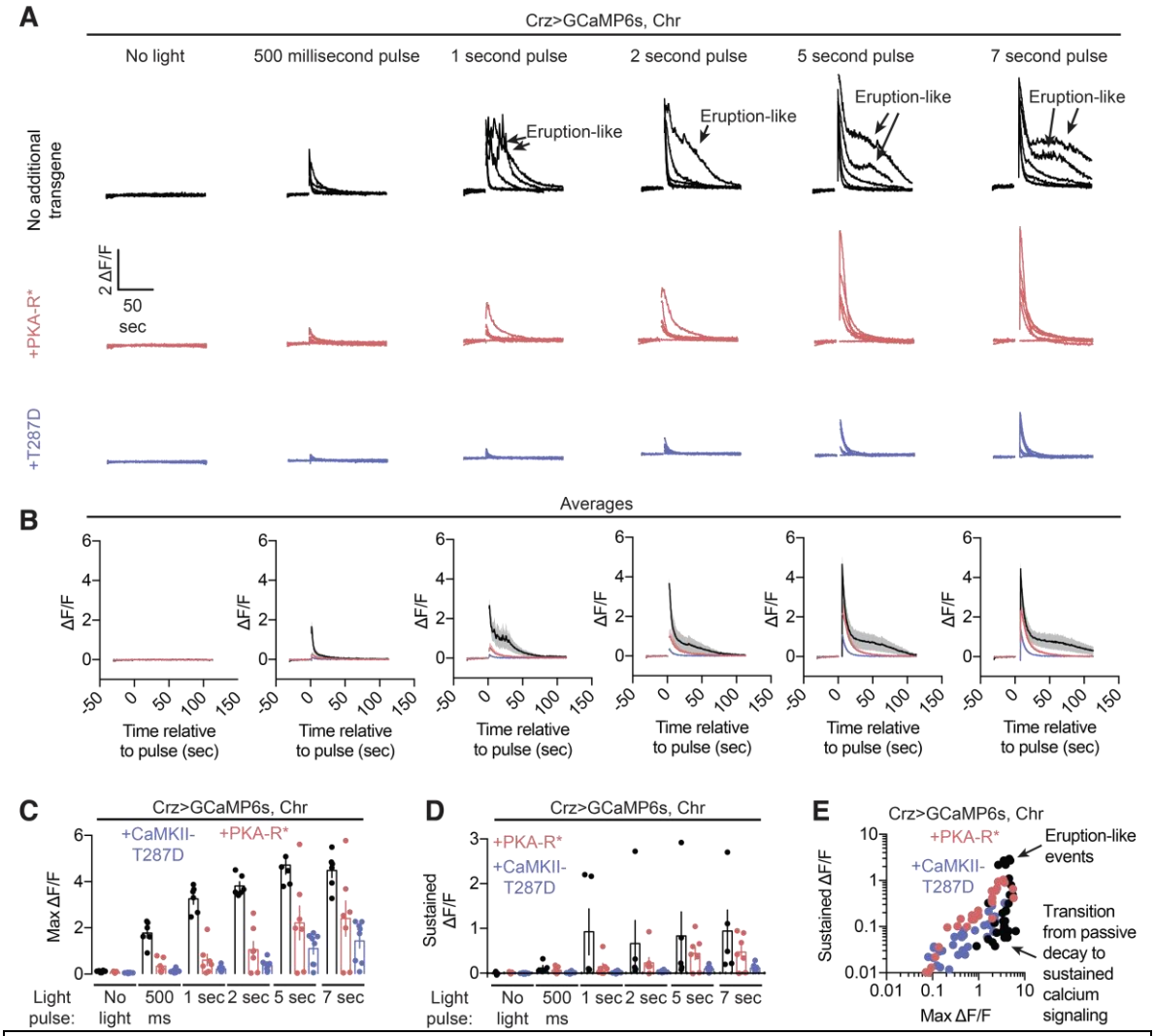

Figure S5 (Related to Figure 4): PKA and CaMKII regulate the magnitude of calcium responses to electrical excitation of the Crz neurons.

A) Individual GCaMP6s responses to optogenetic stimulation of the Crz neurons using CsChrimson.
B) Average of traces in **Figure S5A**.
C) Expression of PKA-R* or CaMKII-T287D attenuate the peak elevation of intracellular calcium levels after electrical excitation of the Crz neurons.
D) Constitutively active CaMKII diminishes the sustained elevation of calcium after stimulation (the average elevation over the period 15-20 seconds after stimulation) (Thornquist et al., 2020) possibly derived from recurrence, while PKA-R* has a less pronounced effect on sustained activity.
E) The relationship between the maximal response of the Crz neurons to the sustained response suggests two regimes: one in which the sustained activity is highly sensitive to changes in maximal excitation (when the maximal activity is high), and one in which it is relatively insensitive (when the maximal activity is low). This is suggestive of a transition into recruiting recurrent excitation when the Crz neurons are driven with a sufficiently strong impulse. Below the threshold, recurrence is not recruited and the residual calcium

presumably results exclusively from the decay of the initial impulse. Arrow points to the abrupt kink in the relationship between peak and sustained fluorescence changes, indicating when sustained calcium begins to grow rapidly with small increases in stimulation strength.

Figure S6

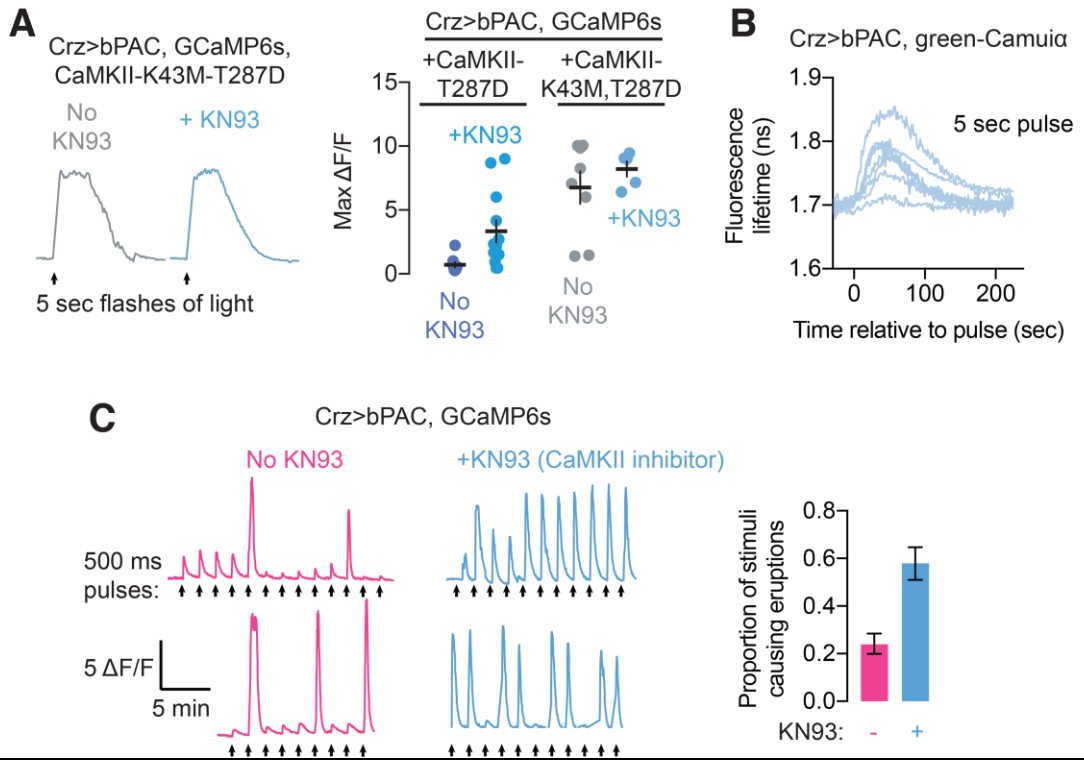

Figure S6 (Related to Figure 6): CaMKII activation after an eruption resets the Crz network

A) Control and summary data for **Figure 6F**. Application of the CaMKII inhibitor KN93 has little effect on the eruption itself in the absence of constitutively active CaMKII.
B) Evoking an eruption with 5 seconds of stimulation of bPAC activates CaMKII as measured by green-Camuiα fluorescence lifetime. The elevation of CaMKII activity is much weaker, and so lasts a shorter duration, than with optogenetic stimulation (Thornquist et al., 2020), suggesting that different sources of intracellular calcium can be more or less effective at driving CaMKII activation, even if they result in similar overall levels of calcium elevation.
C) GCaMP6s fluorescence during repeated stimulation of bPAC in the Crz neurons with and without KN93. Application of KN93 permits eruptions to be elicited one after another, even if pulses of bPAC activation are spaced out by 100 seconds, arguing that CaMKII activation clears out cAMP levels after each eruption.

Figure S7

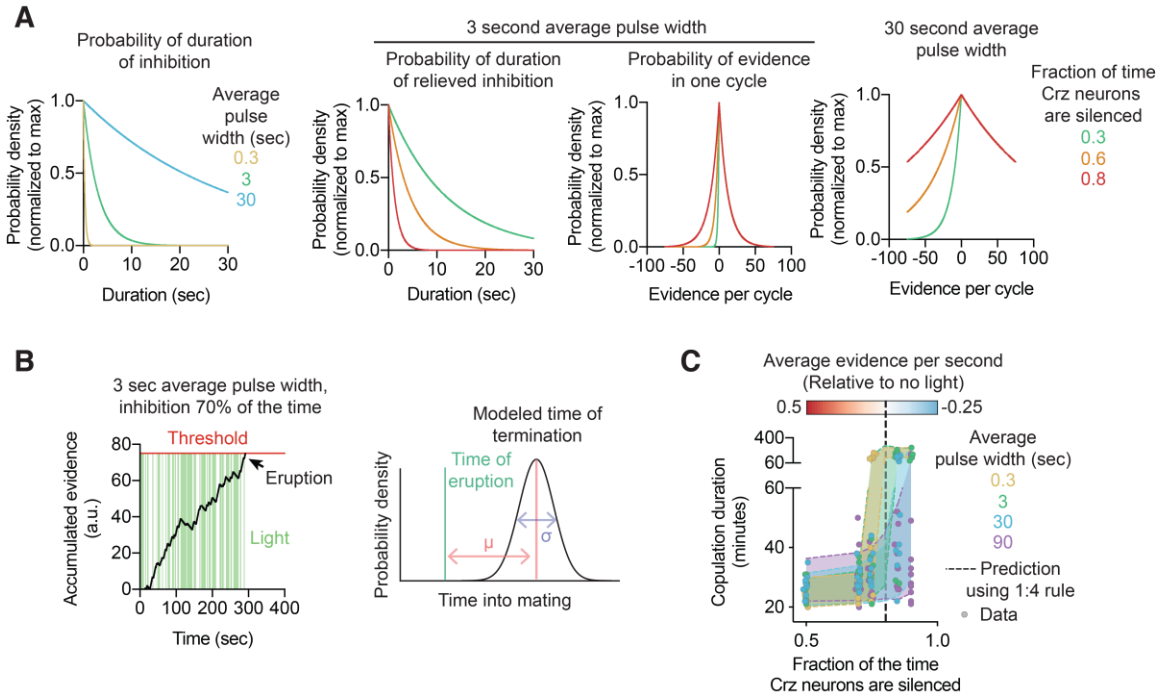

Figure S7 (Related to Figure 7): Details of randomized inhibition experiments

A) Schematic of the distribution of light pulses and relieved inhibition in the experiments in **Figure 7E**.
Left: Probability of each light pulse width is determined by a single parameter: the mean width of a light pulse m. Pulse width is drawn from an exponential distribution with this mean: $P(\text{light pulse width} = \text{t}) = \frac{1}{m}\exp\left(-\frac{t}{m}\right)$
Right: Average duration of relieved inhibition is determined by the mean pulse width m and the fraction of the time the Crz neurons are silenced f: $P(\text{relief width} = \text{t}) = \frac{f}{m(1-f)}\exp\left(-\frac{tf}{m(1-f)}\right)$.
B) Schematized evidence accumulation to threshold to produce a simulated copulation duration. Evidence is accumulated to a threshold (equivalent to 75 seconds of no inhibition), after which a delay until mating termination is drawn from a Gaussian with mean 18 minutes.
C) Comparison between simulated copulation durations as in **Figure S7B** and actual copulation durations. Mean pulse width is indicated by color, while position on the x-axis describes the fraction of the time the Crz neurons are silenced. Dotted lines indicate the 5th-95th percentile copulation durations of simulated data. Individual circles show the copulation durations of single flies.

SUPPLEMENTARY TABLES

Supplementary Table 1: Fly stocks used and origin (Related to STAR Methods)

Stock name (ordered by appearance in main figures)	Origin
Crz-Gal4	BDSC 51976
UAS-GtACR1-eYFP	Adam Claridge-Chang lab
UAS-green-Camuiα	Michael Crickmore lab
UAS-ChR2-XXM	Robert Kittel lab
UAS-Syt-eGFP	BDSC 6926
UAS-DenMark	BDSC 33061
Repo-Gal80	Tzumin Lee lab
Hs-FLP	BDSC 62118
UAS-FRT-STOP-FRT-CsChrimson-tdTomato	David Anderson lab
GCaMP6s	David Anderson lab
Coin-FLP	BDSC 58750
LexAop-FLP	BDSC 55819
Crz-LexA	Michael Crickmore lab
LexAop2-GtACR1-eYFP	Michael Crickmore lab
UAS-Kir2.1-eGFP	BDSC 6595
UAS-Dicer2	BDSC 24646
RNAi and overexpression in Figure 2e	BDSC and VDRC (stock numbers available upon request)
UAS-Gα_s-RNAi	BDSC 50704
UAS-Gα_s-OE	BDSC 6489
UAS-PDE4-RNAi	BDSC 27250
UAS-AC3-OE	BDSC 68221
UAS-bPAC	BDSC 78788 / Robert Kittel lab
UAS-PKA-C1-RNAi	BDSC 31277
UAS-PKA-R*	BDSC 35550
UAS-PKA-mC*	Daniel Kalderon lab
UAS-ASAP2s	BDSC 76247
UAS-Ca-β-RNAi	VDRC 105748
UAS-cADDis$_{Green\text{-}Down}$	Vanessa Ruta lab
UAS-FLIM-AKAR	Michael Crickmore Lab
UAS-CsChrimson-tdTomato	David Anderson lab
UAS-Unc13-RNAi	BDSC 29548
UAS-CaMKII-T287D	Michael Crickmore lab
DIN-Gal4	Kyoto Stock Center 113024
P1-Gal4	BDSC 39599
lLNvs	BDSC 39599
UAS-cADDis$_{Red\text{-}Up}$	Vanessa Ruta lab
UAS-CaMKII-K43M-T287D	Michael Crickmore lab